# $E$ decays to $\eta\pi\pi$ in $\overline{p}p$ annihilation at rest

**Crystal Barrel Collaboration**

C. Amsler[o], D.S. Armstrong[a1], C.A. Baker[e], B.M. Barnett[c], C.J. Batty[e], M. Benayoun[f], K. Beuchert[b], P. Birien[a], P. Blüm[h], R. Bossingham[a], K. Braune[l], J. Brose[k2], D.V. Bugg[i], T. Case[a], A.R. Cooper[i], O. Cramer[l], K.M. Crowe[a], T. Degener[b], H.P. Dietz[l], N. Djaoshvili[f], S. v. Dombrowski[o], M. Doser[f], W. Dünnweber[l], D. Engelhardt[h], M. Englert[l], M.A. Faessler[l], P. Giarritta[o], R. Hackmann[c], R.P. Haddock[j], F.H. Heinsius[a], M. Herz[c], N.P. Hessey[l], P. Hidas[d], C. Holzhaußen[h], P. Illinger[l], D. Jamnik[l3], H. Kalinowsky[c], B. Kalteyer[c], B. Kämmle[g], T. Kiel[h], J. Kisiel[f4], E. Klempt[c], H. Koch[b], C. Kolo[l], M. Kunze[b], M. Lakata[a], R. Landua[f], J. Lüdemann[b], H. Matthäy[b], R. McCrady[m], J.P. Merlo[a], C.A. Meyer[m], L. Montanet[f], A. Noble[o5], R. Ouared[f], F. Ould-Saada[o], K. Peters[b], C.N. Pinder[e], G. Pinter[d], S. Ravndal[b], C. Regenfus[l], E. Schäfer[k6], P. Schmidt[g], M. Schütrumpf[b], I. Scott[i], R. Seibert[g], S. Spanier[o], H. Stöck[b], C. Straßburger[c], U. Strohbusch[g], M. Suffert[n], U. Thoma[c], M. Tischhäuser[h], D. Urner[o7], C. Völcker[l], F. Walter[k], D. Walther[b], U. Wiedner[g], N. Winter[h], J. Zoll[f], B.S. Zou[i], Č. Zupančič.[l]

[a] *University of California, LBL, Berkeley, CA 94720, USA*
[b] *Universität Bochum, D-44780 Bochum, FRG*
[c] *Universität Bonn, D-53115 Bonn, FRG*
[d] *Academy of Science, H-1525 Budapest, Hungary*
[e] *Rutherford Appleton Laboratory, Chilton, Didcot OX11 0QX, UK*
[f] *CERN, CH-1211 Genève, Switzerland*
[g] *Universität Hamburg, D-22761 Hamburg, FRG*
[h] *Universität Karlsruhe, D-76021 Karlsruhe, FRG*
[i] *Queen Mary and Westfield College, London E1 4NS, UK*
[j] *University of California, Los Angeles, CA 90024, USA*
[k] *Universität Mainz, D-55099 Mainz, FRG*
[l] *Universität München, D-80333 München, FRG*
[m] *Carnegie Mellon University, Pittsburgh, PA 15213, USA*
[n] *Centre de Recherches Nucléaires, F-67037 Strasbourg, France*
[o] *Universität Zürich, CH-8057 Zürich, Switzerland*

Received ; revised manuscript received

We have observed the $\eta\pi^+\pi^-$ and $\eta\pi^0\pi^0$ decay modes of the $E$ meson in $\overline{p}p$ annihilation at rest into $\pi^+\pi^-\pi^0\pi^0\eta$. The mass and width of the $E$

The $E$ meson ($M$ = 1425 MeV, $\Gamma$ = 80 MeV), decaying to $K\overline{K}\pi$, was first observed in $\overline{p}p$ annihilation at rest into $K\overline{K}3\pi$ in liquid hydrogen [1]. Its quantum numbers were determined to be $J^{PC}$=$0^{-+}$, the isospin $I = 0$ being favoured over $I = 1$. A fraction of about 50% of the $K\overline{K}\pi$ final

[1]Now at College of William & Mary, Williamsburg,USA
[2]Now at Universität Dresden, Dresden, Germany
[3]University of Ljubljana, Ljubljana, Slovenia
[4]University of Silesia, Katowice, Poland
[5]Now at CRPP, Ottawa, Canada
[6]Now at Max Planck Institute, München, Germany
[7]This work is the PhD thesis of D. Urner

state was found to proceed through the intermediate $K^*\overline{K}$ + c.c. while the remaining 50% was attributed to the intermediate $a_0(980)(\rightarrow K\overline{K})\pi$. The Asterix Collaboration at LEAR has also observed an enhancement at 1413 MeV in $\overline{p}p$ annihilation at rest into $K^{\pm}(K^0)_{miss}\pi^{\mp}\pi^+\pi^-$ in gaseous hydrogen [2]. A spin-parity analysis was not performed due to limited statistics. The weaker $E$ production in gas than in liquid is, however, consistent with the emission of a $0^{-+}$ state from atomic S orbitals, which are less populated in gas. A $0^{-+}$ signal in $K\overline{K}\pi$ was also reported in $\overline{p}p$ annihilation at 6.6 GeV/c [3]. The $0^{-+}$ spin-parity assignment to the $E$ meson has nevertheless remained controversial, various experiments in other hadronic reactions reporting a $1^{++}$, $f_1(1420)$, and/or a $0^{-+}$, $\eta(1440)$, in this mass region [4].

A $0^{-+}$ state decaying to $K\overline{K}\pi$, named $\iota$, was also observed in radiative $J/\psi$ decay [5]. This state was interpreted as a prominent glueball candidate due to its strong production in a gluon rich channel. More recent data from the Mark III collaboration [6] suggest three overlapping resonances in this mass region, a $0^{-+}$ around 1416 MeV decaying to $a_0(980)\pi$, a $1^{++}$ at 1443 MeV and a $0^{-+}$ around 1490 MeV decaying into $K^*(892)\overline{K}$. This raises the possibility that the 1416 MeV state in the $\iota$ structure and the $E$ meson, if $0^{-+}$, are actually identical. A substructure in the $E/\iota$ region is also observed in radiative $J/\psi$ decay by DM2 [7] and in $\overline{p}p$ annihilation at rest by the Obelix Collaboration at LEAR [8].

The $\eta\pi\pi$ decay mode may help to disentangle a $0^{-+}$ from a $1^{++}$ state. From the $a_0(980)\pi \rightarrow K\overline{K}\pi$ decay modes of the $E$ meson and the lower state in the $\iota$ structure one would expect a prominent signal in the final state $a_0\pi \rightarrow \eta\pi\pi$. This has indeed been observed by DM2 [9] and Mark III [10] in radiative $J/\psi$ decay. An $\eta\pi\pi$ structure was observed at 1400 MeV in $\overline{p}p$ annihilation at 700 MeV/c [11] but no spin-parity analysis was performed. In contrast, no $\eta\pi\pi$ signal is seen in $f_1(1420)$ decay [12].

In this letter we report the first observation of the $E$ meson decaying to $\eta\pi^+\pi^-$ and $\eta\pi^0\pi^0$ in $\overline{p}p$ annihilation at rest into $\pi^+\pi^-\pi^0\pi^0\eta$, leading to $\pi^+\pi^-$ and 6 detected photons. A spin-parity analysis was performed with the aim (i) to firmly establish that $E$ is pseudoscalar, (ii) to measure the relative contributions of $a_0\pi$ and $\eta(\pi\pi)_s$ decays (where $(\pi\pi)_s$ is an S-wave dipion) and (iii) to determine whether the $E$ meson and the lower state in the $\iota$ structure are identical.

The experiment was performed at the Low Energy Antiproton Ring (LEAR) at CERN. A detailed description of the apparatus can be found in ref. [13]. Antiprotons with a momentum of 200 MeV/c are stopped in a 4 cm long liquid hydrogen target. The antiproton beam is defined by a proportional wire chamber, a matrix of four silicon counters and a small 5 mm diameter circular silicon counter which further restricts the incident beam size on the hydrogen target. The target is surrounded by two cylindrical proportional wire chambers, a jet drift chamber (JDC) to detect charged particles and a barrel-shaped calorimeter consisting of 1380 CsI(Tl) crystals with photodiode readout. The assembly is located in a solenoid providing a homogeneous field of 1.5 T parallel to the incident antiproton beam.

The JDC covers a solid angle of 94% $\times 4\pi$ for the innermost and 64% $\times 4\pi$ for the outermost of the 23 layers. It is cylindrical with a length of 40 cm and a diameter of 51 cm and is divided into 30 azimuthal sectors. The coordinate along the beam axis is measured by charge division. We use slow gas, a mixture of 90% carbon dioxide and 10% isobutane at atmospheric pressure. The momentum resolution achieved for the present data is about $\sigma/p$ = 2.5 % for charged pions at 200 MeV/c, rising to about 4 % at 600 MeV/c.

The CsI calorimeter covers the polar angles between 12° and 168° with full coverage in azimuth. The crystal information is read out by two ADC systems in parallel, one providing a high sensitivity over a limited range (0 to 400 MeV), the other (0 to 2000 MeV) also providing a fast readout for the trigger system (see below). The $\gamma$ energy resolution is $\sigma/E$ = 2.5 % for 1 GeV photons and the angular resolution is typically $\sigma$ = 20 mr in both polar and azimuthal angles.

The minimum bias trigger (first trigger level) requires an incident $\overline{p}$, *i.e.* a coincidence between the beam-defining silicon and any of the four other silicon counters. In view of the expected low branching ratio for the $E$ signal we collected the present data with a trigger selecting $\pi^+\pi^-\pi^0\pi^0\eta$ events. The optimum trigger parameters were obtained by submitting minimum bias events, which were reconstructed offline as $\pi^+\pi^-\pi^0\pi^0\eta$ events, to a trigger simulator or by replaying them through the online software trigger. The goal was to maximize the enrichment factor (the fraction of reconstructable $\pi^+\pi^-\pi^0\pi^0\eta$ events on tape) and the data acquisition speed.

The second trigger level selects the charged multiplicity from the JDC and rejects pile-up events. The trigger information is extracted from layers 2-5 for which we accept events with 2 hits in each of the 4 layers. To increase the offline reconstruction efficiency and improve on the momentum resolution we ask for 2 long tracks (2 hits in layer 20 and 2 hits in layer 21). The decision time of the second trigger level is 6 $\mu s$. The enrichment factor is 6.3 (which includes the 2-prong branching ratio of about 45%). The trigger efficiency for $\pi^+\pi^-\pi^0\pi^0\eta$ is 18% due to the restricted solid angle and small inefficiencies of the JDC readout (from which we require exactly 2 hits on 6 layers).

The third trigger level uses a fast cluster encoding processor which counts the number of clusters registered in the calorimeter: the crystals are mapped onto a matrix of 26 rows and 60 columns. For all crystals with energy deposits above threshold (here 18 MeV) the corresponding bit in the matrix is set. A hardwired algorithm then finds clusters of neighbouring bits. Since we require two charged particles and six photons, we ask for exactly eight clusters in the barrel. The total energy deposit in the barrel is also required to lie between 950 and 1700 MeV. The decision time is 43 $\mu$s, the enrichment factor 4.4 and the efficiency 63%.

The fourth trigger level (software trigger) then receives the energy information from the fast conversion ADC's, finds the clusters and computes the energy deposits in the clusters. The center of the cluster is determined by the crystal with the highest energy deposit. The trigger can separate two clusters if there is a gap with energy deposition below a given threshold (13 MeV for the present data). Clusters with less than a given minimum (18 MeV for the present data) are ignored. The software trigger needs 300 $\mu s$ to calculate the number of clusters.

In the next step the invariant masses of all possible $\gamma$- pair combinations are calculated. We define $\pi^0$ and $\eta$ mass windows as 121 to 149 MeV and 529 to 578 MeV, respectively, and accept at most one combination outside the $\pi^0$ and $\eta$ windows (to allow for the energy deposits of the charged pions) and require at most $2\pi^0$ or $2\eta$ [1]. The decision time lies between 1 and 2 ms. The enrichment factor of the software trigger is 3.5 and the efficiency 44%.

We then obtain a total enrichment of 97 and a total trigger efficiency of 5%. The data acquisition rate saturates at 25 Hz for about $3 \times 10^4$ incident $\overline{p}$/s, compared to 40 Hz for minimum bias events. The present data ($5.83 \times 10^6$ triggered events) were collected in 8 days.

After event reconstruction by the offline analysis we require two tracks with opposite charges, each with at least 15 wires hit. This leaves a sample of $5.16 \times 10^6$ events. Crystals with energy deposits below 1 MeV are ignored and clusters are required to have at least 20 MeV. A cluster originating from a charged particle is discarded as a $\gamma$ candidate if the extrapolated trajectory from the JDC matches a cluster in the barrel. Unmatched energy deposits arise either from photons or from secondary hadron interactions in the barrel (split-offs). Events with at least 6 and at most 8 unmatched clusters (thus allowing for at most 2 split-offs) are submitted to a 4C kinematic fit to the final state $\pi^+\pi^-6\gamma$, requiring total momentum and total energy conservation. The most likely $6\gamma$ combination is obtained by fitting all combinations and retaining the combination with the highest confidence level. This leaves $3.30 \times 10^6$ events with a confidence level of more than 1%. We find that 58% of the fitted $\pi^+\pi^-6\gamma$ events have 0, 29% have 1 and 13% have 2 split-offs in the barrel.

The events are then submitted to a 7C kinematic fit imposing the $\pi^0$ and $\eta$ masses: events satisfying the $\pi^+\pi^-\pi^0\pi^0\eta$ hypothesis with a confidence level larger than 20% and failing both the $\pi^+\pi^-3\pi^0$ and $\pi^+\pi^-\pi^0\eta\eta$ fits with each more than 99% probability are retained for further analysis. Ambiguous events with more than one $2\pi^0\eta$ combination with a confidence level larger than 1%

[1] The $2\eta$ selection is used to study in parallel the final state $\pi^0\eta(\eta' \to \eta\pi^+\pi^-)$ [14].

are also rejected. This leaves a sample of 298'508 $\pi^+\pi^-\pi^0\pi^0\eta$ events. The $\eta\pi^0\pi^0$ and $\eta\pi^+\pi^-$ mass distributions are shown in fig. 1. Apart from the strong $\eta'$ signals one observes a shoulder in $\eta\pi^0\pi^0$ and an enhancement in $\eta\pi^+\pi^-$ in the 1400 MeV region, presumably due to the $E$-meson.

Figure 2 shows the $\pi^+\pi^-\pi^0$ and $\pi^0\eta$ mass distributions with clear evidence for the $\pi^0\eta\omega$ and $\pi^0\eta\eta$ channels. The most prominent contribution to $\pi^0\eta\omega$ is the intermediate $a_0(980)\omega$ (fig. 2a). An 8C kinematic fit leads to 131'370 $\pi^0\eta\omega$ events with a confidence level of more than 20%. The Dalitz plot of these events [15] is identical to the one observed in the final state $\pi^0\eta\omega \to 7\gamma$ studied earlier by our collaboration. We found that $a_0(980)\omega$ contributes about 50% to $\pi^0\eta\omega$ [16].

To simplify the further analysis all events compatible with $\pi^0\eta\omega(\to \pi^+\pi^-\pi^0)$ or $\pi^0\eta\eta(\to \pi^+\pi^-\pi^0)$ with a confidence level of more than 1% are removed. This then leaves a sample of 126'866 events. The resulting $\eta\pi\pi$ mass distributions and the clear signals for the $E$ meson decaying to $\eta\pi^0\pi^0$ and $\eta\pi^+\pi^-$ are shown in fig. 3. We estimate the number of visible $E$ mesons to be about 9000. To study further the $E$ signal one could remove events in the $\eta'$ peaks, but in contrast to the $\omega$ events which are broadly distributed in the $\eta\pi\pi$ mass distribution, the $\eta' \to \eta\pi^0\pi^0$ events generate a broad reflection in the 1400 MeV $\eta\pi^+\pi^-$ region and, conversely, the $\eta' \to \eta\pi^+\pi^-$ events in the 1400 MeV $\eta\pi^0\pi^0$ mass region. This cut is therefore not applied.

We now determine the branching ratio for the annihilation channel $\bar{p}p \to \pi^+\pi^-\pi^0\pi^0\eta$ using two different methods. We first calculate the branching ratio for $\pi^+\pi^-\pi^0\pi^0\eta$, relative to that for $\pi^+\pi^-3\pi^0$, by submitting a sample of $1.23 \times 10^5$ minimum bias events to the same offline analysis. We obtain $75\pm9$ $\pi^+\pi^-\pi^0\pi^0\eta$ events and $687\pm26$ $\pi^+\pi^-3\pi^0$ events. The detection and reconstruction efficiency is determined by Monte-Carlo simulation of the detector and data reduction procedure using GEANT [17], assuming phase space distribution. We find a detection and reconstruction efficiency of (10.3 $\pm$ 0.2) % and (10.6 $\pm$ 0.2) % for minimum bias $\pi^+\pi^-\pi^0\pi^0\eta$ and $\pi^+\pi^-3\pi^0$ events, respectively. Since systematic errors largely cancel in the ratio we quote statis-

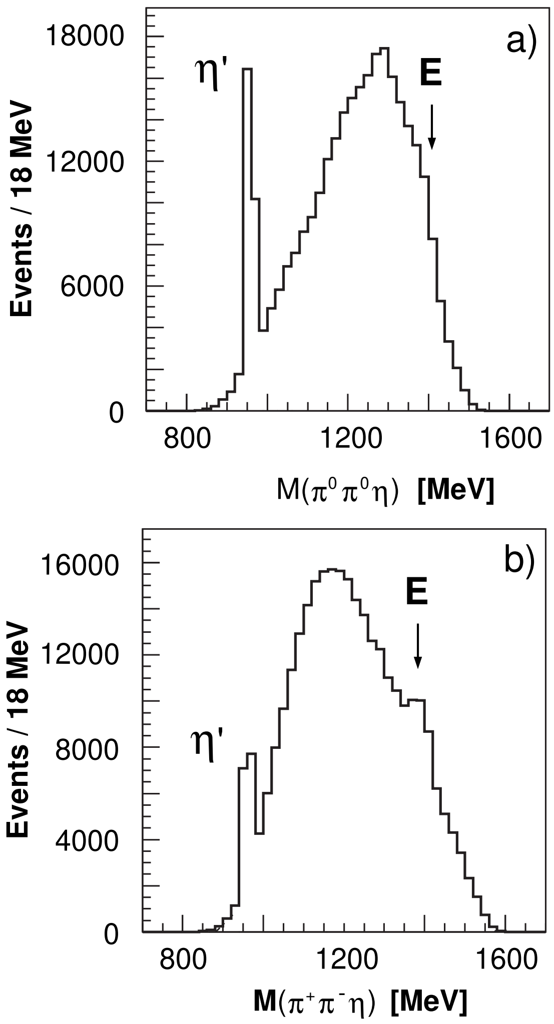


Fig. 1. $\eta\pi^0\pi^0$ (a) and $\eta\pi^+\pi^-$ (b) mass distributions of $\pi^+\pi^-\pi^0\pi^0\eta$ events.

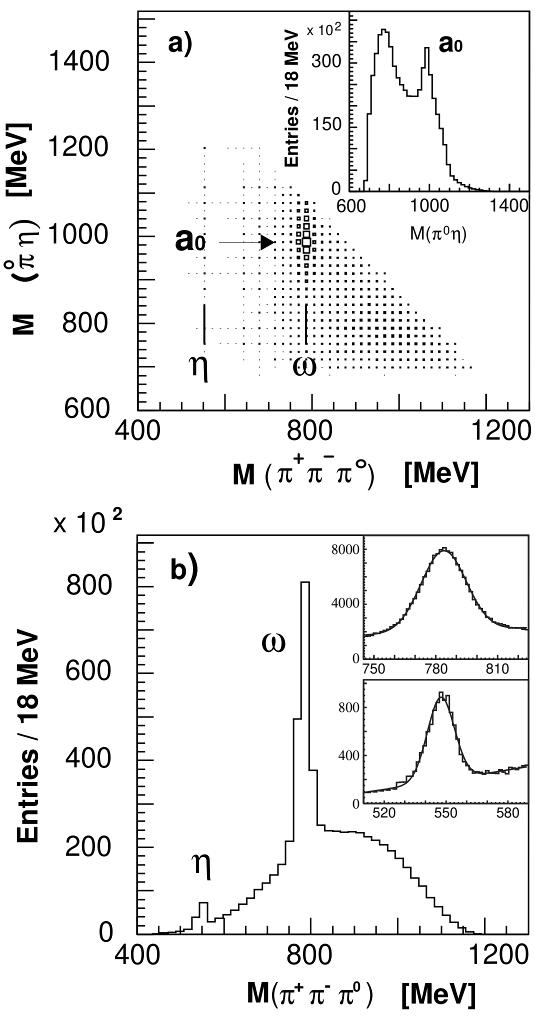


Fig. 2. a): $\pi^0\eta$ vs $\pi^+\pi^-\pi^0$ mass scatterplot (2 entries/event). The inset shows the $\pi^0\eta$ mass projection. The $a_0(980)$ peak comes dominantly from the annihilation channel $a_0\omega$. b): $\pi^+\pi^-\pi^0$ mass distribution (2 entries/event). The insets show the fits to the $\omega$ and $\eta$ regions (Gaussians with polynomial backgrounds)

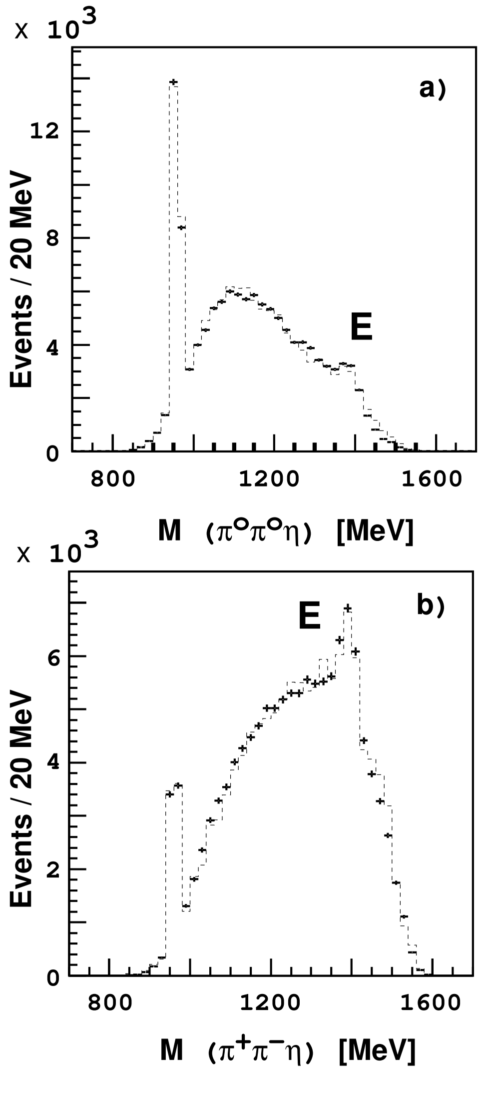


Fig. 3. $\eta\pi^0\pi^0$ (a) and $\eta\pi^+\pi^-$ (b) invariant mass distributions after removal of the $\pi^0\eta\omega$ and $\pi^0\eta\eta$ contributions to $\pi^+\pi^-\pi^0\pi^0\eta$ . The data are shown with error bars. The dashed lines show the result of fit B described below.

tical errors only. Using the branching ratio for $\pi^+\pi^-3\pi^0$ determined earlier by our collaboration, (9.7 ± 0.6) % [18], and taking into account the known $2\gamma$ decay branching ratio of $\pi^0$ and $\eta$, we find $B(\pi^+\pi^-\pi^0\pi^0\eta) = (2.78 \pm 0.40)$ % where the uncertainty is dominated by the statistical error for the minimum bias $\pi^+\pi^-\pi^0\pi^0\eta$ sample.

Using the second method we extract from our triggered data sample 101'520 ± 1440 $\pi^0\eta\omega(\rightarrow \pi^+\pi^-\pi^0)$ and 7'155 ± 253 $\pi^0\eta\eta(\rightarrow \pi^+\pi^-\pi^0)$ events by fitting Gaussians with polynomial backgrounds to the $\omega$ and $\eta \rightarrow \pi^+\pi^-\pi^0$ mass distributions (fig.2b). The corresponding detection and reconstruction efficiencies are determined by generating a sample of $5.8\times10^6$ phase space distributed $\pi^+\pi^-\pi^0\pi^0\eta$ GEANT events which are submitted to a trigger simulator and then processed through the same offline analysis as real events. This data sample will also be used below to perform the amplitude analysis of the $E$ meson. We obtain an efficiency of (2.3 ± 0.2) % for $\pi^0\eta\omega$ and (1.8 ± 0.1) % for $\pi^0\eta\eta$. The lower efficiency compared to minimum bias data is due to the trigger efficiency.

The branching ratios for the channels $\pi^0\eta\omega$, (0.68 ± 0.05 )%, and $\pi^0\eta\eta$, (0.21± 0.04) %, have been measured by our collaboration in the all-neutral $7\gamma$ and $6\gamma$ final state [16,19]. With our 298'508 $\pi^+\pi^-\pi^0\pi^0\eta$ events (reconstruction efficiency (2.30 ± 0.03) %) we then obtain $B(\pi^+\pi^-\pi^0\pi^0\eta) = (1.78 \pm 0.21)$ % and (3.24 ± 0.65) %, taking into account the known decay branching ratios for $\omega$ and $\eta$ (and a factor of two for $\pi^0\eta\eta$). These numbers are in reasonable agreement with the determination above, (2.78 ± 0.40) %, and provide a consistency check within the Crystal Barrel measurements. Averaging and increasing the errors with the standard Rosenfeld method [4] we find

$$B(\pi^+\pi^-\pi^0\pi^0\eta) = (2.09 \pm 0.36)\%, \quad (1)$$

which will be used below to calculate the branching ratio for $E$ production.

We now proceed to the spin-parity analysis of the $\pi^+\pi^-\pi^0\pi^0\eta$ final state, excluding the $\omega$ and $\eta \rightarrow \pi^+\pi^-\pi^0$ contributions, which leaves 126'866 events. The data are analyzed with a maximum likelihood fit using the helicity formalism [20] in the isobar model, in which the initial $\bar{p}p$ system is assumed to decay to the $\pi^+\pi^-\pi^0\pi^0\eta$ final state through two-body intermediate states. The two-body decay amplitude is given by the matrix

$$\begin{aligned} A &= D^J_{\lambda M}(\theta,\phi)F_L(q)BW_L(m) \\ &\times \langle J\lambda \mid LS0\lambda\rangle\langle S\lambda \mid S_1S_2\lambda_1,-\lambda_2\rangle. \end{aligned} \quad (2)$$

The row index $\lambda = \lambda_1 - \lambda_2$ runs over the $(2S_1 + 1)(2S_2 + 1)$ daughter helicities, while the column index $M$ runs over the $(2J + 1)$ magnetic substates of the isobar; $q$ is the daughter momentum and $\theta$ and $\phi$ refer to the decay angles in the isobar rest frame. $BW_L(m)$ is the Breit-Wigner amplitude for the isobar, and $F_L$ are damping factors. For the $\eta'$ we use a Gaussian since the width is determined by the resolution of the apparatus. For the $\pi\pi$ S- wave we replace the Breit-Wigner amplitude by the S-wave amplitude measured in elastic $\pi\pi$ scattering [21]. More details on the formalism can be found in our analysis of the $\omega\pi^0\pi^0$ channel [22].

The total amplitude $A_{jl}$ for a decay chain l and a $\pi^+\pi^-\pi^0\pi^0\eta$ event j is a product of matrices $A$ (eqn. 2). We assume S-state annihilation dominance following capture in liquid hydrogen [23] and use only contributions from the S-states of the $\bar{p}p$ atom to $\pi^+\pi^-\pi^0\pi^0\eta$. The various chains are added coherently if they have the same initial state: ${}^1S_0[I^G(J^{PC}) = 0^+(0^{-+})]$ or ${}^3S_1[I^G(J^{PC}) = 1^+(1^{--})]$. The fits are repeated for various fixed resonance masses and widths.

The quantity to be minimized is

$$S = 2N\ln\sum_{i=1}^{M} w_i(MC) - 2\sum_{i=1}^{N}\ln w_i(DAT) \quad (3)$$

where $w_i(MC)$ and $w_i(DAT)$ are weights calculated for Monte Carlo and data events, respectively. The sums run over N data events and M Monte Carlo events. The weights are given by

$$\begin{aligned} w_j &= \left|\sum_{l=1}^{L_1} a_l e^{-i\phi_l} A_{jl}({}^1S_0)\right|^2 \\ &+ \left|\sum_{l=1}^{L_2} a'_l e^{-i\phi'_l} A_{jl}({}^3S_1)\right|^2, \end{aligned} \quad (4)$$

with appropriate normalization of the amplitudes

$$A_{jl} \to \frac{A_{jl}}{\sqrt{\sum_{i=1}^{M} |A_{il}|^2}}. \tag{5}$$

$L_1$ and $L_2$ are the numbers of chains leading to the observed final state. The real parameters $a_l$, $a'_l$, $\phi_l$ and $\phi'_l$ are determined by the fit. For each initial state the phase $\phi$ of one decay chain is arbitrary and set to zero. There are sometimes two possibilities to form a given decay chain, for example $X \to \pi^+ a_0^-$ and $X \to \pi^- a_0^+$. In this case the amplitudes $a_1$ and $a_2$ are equal but $\phi_1 = \phi_2$ for isoscalar and $\phi_1 = \phi_2 + \pi$ for isovector decay.

Before fitting the $E$ we try a series of "background" chains to describe the $\pi^+\pi^-\pi^0\pi^0\eta$ final state without the $E$ signal. We neglect contributions from channels with $\pi\pi$ in a relative D wave (*e.g.* $f_2(1270)$) and $\pi\eta$ in a relative D wave (*e.g.* $a_2(1320)$). This is justified by the absence of obvious signal and the lack of phase space for these excitations at rest.

From the $^1S_0$ initial state we include direct contributions from $0^{++}\eta$ where the four-pion $0^{++}$ system decays to $\sigma^{+-}\sigma^0$ and $\rho^+\rho^-$. Here $\sigma^{+-}$ stands for the $\pi^+\pi^-$ S-wave and $\sigma^0$ for the $\pi^0\pi^0$ S-wave [21]. By direct contribution we mean that the four-pion resonance is very broad and thus we set $BW$=1. We also include $\eta'\sigma^0$ and $\eta'\sigma^{+-}$, using for $\eta' \to \eta\pi\pi$ three-body phase space since the $\eta'$ decay Dalitz plot is, to a very good approximation, entirely flat [24,25].

From the $^3S_1$ initial state we include the $\eta'\rho^0$ amplitude and direct contributions from (i) $1^{--}\eta$ where the four-pion system decays to $\rho^0\sigma^0$ with angular momenta 0 or 2, (ii) $[1^{--} \to \eta\rho^0]\sigma^0$, (iii) $[1^{+-} \to \eta\rho^0, a_0^{\pm}(980)\pi^{\mp}]\sigma^0$ and (iv) $[0^{-+} \to \eta\sigma^0, a_0^0(980)\pi^0]\rho^0$.

These contributions provide a reasonable description of the background outside the $E$ meson region. Other ingredients, some of which are discussed below, were also introduced into the fit but they did not change the background description significantly. The relative intensities are given in Table 1 (Fit A). Due to large overlaps beween the amplitudes we do not consider the individual intensities for the direct contributions (D.C.) as meaningful quantities and therefore we do not quote them separately in Table 1.

Table 1
Fractional contributions $a_l^2$ to the final state $\pi^+\pi^-\pi^0\pi^0\eta$ (excluding $\pi^0\eta\omega$ and $\pi^0\eta\eta$ contributions). The errors are statistical only. Fit A: background only; fit B: with a $0^{-+}$ $E$; fit C: with a $1^{++}$ $E$; fit D: with both $0^{-+}$ and $1^{++}$ contributions. $\Delta S$ denotes the change in $S$ compared to fit A ($S$=2'909'528). The numbers in square brackets are the intensities with $\eta'$ events removed (normalized to the full data sample). D.C. denotes the sum of the direct contributions.

| | A | B | C | D |
|---|---|---|---|---|
| $\Delta S$ | | -8109 | -1444 | -8248 |
| $^1S_0$ | | | | |
| D.C. | 0.443 | 0.382± 0.015 [0.359] | 0.545 | 0.355 |
| $\sigma^0\eta'$ | 0.041 | 0.041± 0.005 | 0.052 | 0.039 |
| $\sigma^{+-}\eta'$ | 0.087 | 0.091± 0.007 | 0.117 | 0.104 |
| $E(0^{-+})$ | | | | |
| $\to \eta\sigma^0$ | | 0.020± 0.003 [0.020] | | 0.018 |
| $\to \eta\sigma^{+-}$ | | 0.027± 0.004 [0.026] | | 0.033 |
| $\to a_0^0\pi^0$ | | 0.025± 0.004 [0.028] | | 0.025 |
| $\to a_0^{\pm}\pi^{\mp}$ | | 0.035± 0.005 [0.039] | | 0.035 |
| $E(1^{++})$ | | | | |
| $\to \eta\sigma^0$ | | | 0.000 | 0.002 |
| $\to \eta\sigma^{+-}$ | | | 0.001 | 0.003 |
| $\to a_0^0\pi^0$ | | | 0.012 | 0.000 |
| $\to a_0^{\pm}\pi^{\mp}$ | | | 0.004 | 0.001 |
| $^3S_1$ | | | | |
| $\eta'\rho^0$ | 0.020 | 0.022± 0.003 | 0.035 | 0.027 |
| D.C. | 0.410 | 0.358± 0.014 [0.28] | 0.234 | 0.358 |

We then introduce the annihilation channels

$$\begin{array}{lll} \overline{p}p \rightarrow & E & \sigma^{+-} \\ & E & \rightarrow \eta\sigma^{0} \text{and } E \rightarrow \ a_0^0(\rightarrow \eta\pi^0)\pi^0, \\ \overline{p}p \rightarrow & E & \sigma^{0} \\ & E & \rightarrow \eta\sigma^{+-} \text{and } E \rightarrow \ a_0^{\pm}(\rightarrow \eta\pi^{\pm})\pi^{\mp}, \end{array} \quad (6)$$

which only occur from $^1S_0$ atomic orbitals for a $0^{-+}$ $E$ (fit B) or for a $1^{++}$ $E$ (fit C). The amplitudes are added coherently to the background amplitudes from $^1S_0$. Fit B leads to a reduction of $S$ by 8109 compared to 1444 for fit C (Table 1). For fit C we find only a broad minimum around 1410 MeV for which it is not possible to determine the width.

If one introduces both $0^{-+}$ and $1^{++}$ (fit D) $S$ decreases only by 139 with respect to fit B and the $1^{++}$ has a total intensity of $(0.6 \pm 0.1)$ %. The $0^{-+}$ contribution remains stable. The strength of the $1^{++}$ contribution does not depend strongly on the description of the background. Including additional background chains [15] we estimate the $1^{++}$ contribution to be $(0.6 \pm 0.4)$ %, compatible with zero. On the other hand, the $0^{-+}$ contributes $(11.1 \pm 0.8)$ % to the $\pi^+\pi^-\pi^0\pi^0\eta$ final state. We therefore conclude that $E$ is pseudoscalar. Since $E$ decays to $\eta\pi^0\pi^0$ its isospin is zero and its C-parity is C=+1. The fitted $\eta\pi\pi$ mass distributions (fit B) are compared to data in fig. 3.

To illustrate the strong $0^{-+}$ preference we show in fig. 4 the measured angular distributions in the $E$ rest frame, together with the fitted angular distributions for $\sigma^{+-}$ (recoiling against $\eta$ with respect to the flight direction of $E$) and for $a_0^{\pm}$ (recoiling against $\pi^{\mp}$) for fit B and the prediction for a $1^{++}$ $E$ of the same intensity. To enhance the $E$ signal in fig. 4 we have selected events with an $\eta\pi\pi$ mass between 1367 and 1447 MeV and have removed all $\eta'$ events. The $1^{++}$ assignment clearly disagrees with data.

Figure 5 shows the $\eta\pi^{\pm}$ mass distribution in the $E$ region (1367-1447 MeV). A strong $a_0^{\pm}(980)$ peak is observed. The inset shows the $\eta\pi^{\pm}$ mass distribution when events in the side bins of the $E$ meson are subtracted. The strong enhancement around 1000 MeV proves that $E$ indeed decays to $a_0^{\pm}\pi^{\mp}$. The $\eta\pi^0$ spectrum looks similar.

One expects the annihilation rates into $(0^{-+} \rightarrow$

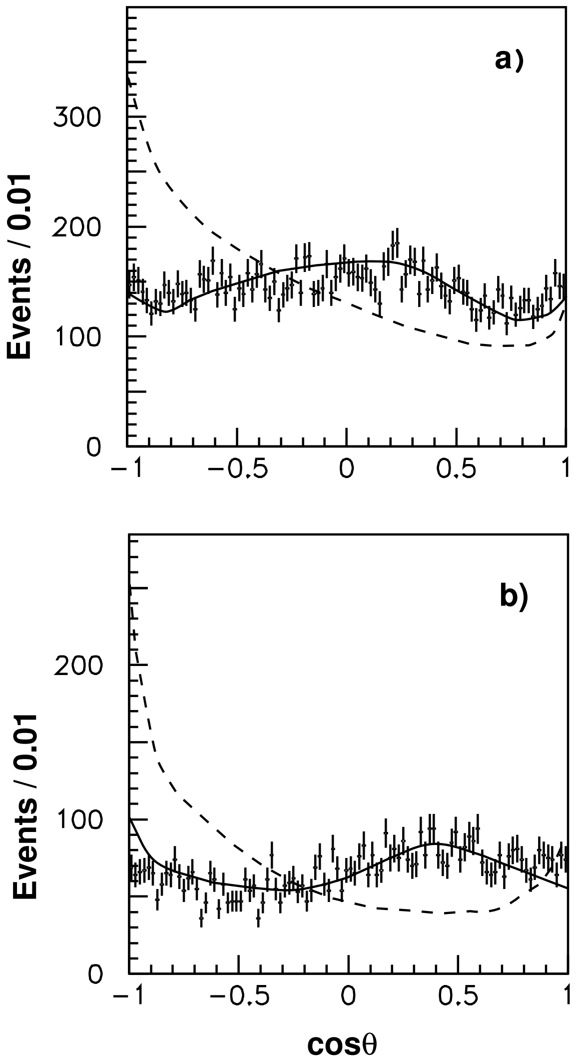


Fig. 4. Angular distributions of the $\sigma^{+-}$ (a) and $a_0^{\pm}$ (b) in the $E$ rest frame. The data are shown with error bars. The lines are smooth interpolations between the fitted Monte Carlo data points. The solid lines show the $0^{-+}$ $E$ contribution (fit B), the dashed lines the predictions when the $0^{-+}$ is replaced by a $1^{++}$ of the same intensity.

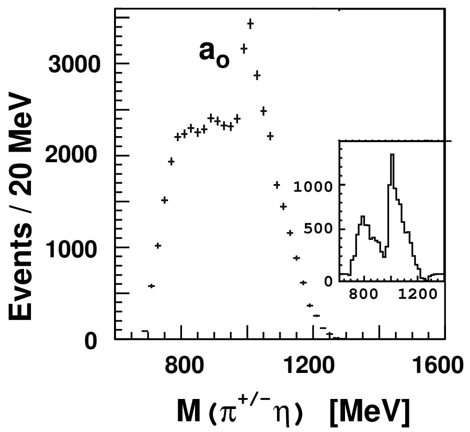


Fig. 5. $\eta\pi^{\pm}$ mass distributions for events in the $E$ region. The inset shows the $E$ side-bin subtracted $a_0^{\pm}$ region.

$\eta\pi^0\pi^0)\pi^+\pi^-$ and $(0^{-+} \rightarrow \eta\pi^+\pi^-)\pi^0\pi^0$ to be equal. Our rates for $E$ decay are indeed comparable but the rate for $\eta' \rightarrow \eta\pi^+\pi^-$ is lower than that for $\eta' \rightarrow \eta\pi^0\pi^0$ (Table 1). The former has, however, a large systematic error due to acceptance limitations for charged pions from $\eta'$ decay which are emitted with very small transverse momenta. To investigate possible effects on the $E$ analysis we remove events in both $\eta'$ regions and repeat the spin-parity analysis. The intensities in brackets (Table 1) have been normalized to the full data set (126'866 events) to allow a direct comparison with fit B. They agree within errors with those of fit B. This means that the $E$ analysis does not depend on details of the $\eta'$ regions.

Further tests were performed by varying the background description *i.e.* by including other chains in fit B. The rates for the $E$ meson were not affected significantly. The $\eta(1295)$ was added and treated analogously to the $E(0^{-+})$. This led to a reduction of $S$ by 279. The $a_2(1650)$ decaying to $\pi\eta'$, reported by our collaboration [26], led to a reduction of 356. Our data are therefore compatible with these states but we do not consider their contributions as significant.

Replacing the direct $0^{-+}\rho^0$ by an $E(0^{-+})\rho^0$ contribution increases $S$ by 1420. Therefore we do not reproduce the small $E\rho^0$ contribution from $^3S_1$ that was reported in ref. [1]. Introducing $\rho(1400) \rightarrow \eta\rho^0$ and $\rho^0\sigma^0$ with a width of 320 MeV instead of the direct $1^{--}$ contributions increases $S$ by 356. Replacing the direct $1^{+-}$ by $b_1(1235)$ increases $S$ by 3906. Replacing the direct $0^{++}$ with the $f_0(1365)$ [18] also increases $S$ by 5560. Our data are therefore not compatible with a contribution from $b_1(1235)$ or $f_0(1365)$ to $\pi^+\pi^-\pi^0\pi^0\eta$.

The mass and width of the $E$ meson are determined by running a large number of fits, varying mass and width by hand. From fit B we obtain

$$\begin{aligned} m(E) &= 1409 \pm 3 \text{ MeV} \\ \Gamma(E) &= 86 \pm 10 \text{ MeV}, \end{aligned} \qquad (7)$$

dominated by systematic errors. The total $E$ contribution to $\pi^+\pi^-\pi^0\pi^0\eta$ is $(10.7 \pm 0.8 \pm 1.8)\%$ (Fit B, Table 1). The systematic errors are estimated from the stability of the results when varying the background description.

From Table 1, one obtains the ratio

$$\frac{B(E \rightarrow \eta(\pi\pi)_s)}{B(E \rightarrow a_0\pi, a_0 \rightarrow \eta\pi)} = 0.78 \pm 0.12 \pm 0.10. \qquad (8)$$

This is compatible with the corresponding DM2 result for their 1398 MeV state, $0.25 \pm 0.34$ [9], if we assume that their observed contribution to $\eta\pi^+\pi^-$, not proceeding through $a_0\pi$, is $\eta(\pi^+\pi^-)_s$.

The branching ratio for $\overline{p}p \rightarrow \pi^+\pi^-\pi^0\pi^0\eta$ is given above (eqn. 1). Subtracting the contributions from $\pi^0\eta\omega$ and $\pi^0\eta\eta$ one finds $(1.39 \pm 0.36)$ % which then leads to the absolute branching ratio

$$B(\overline{p}p \rightarrow E\pi\pi)B(E \rightarrow \eta\pi\pi) = (3.3 \pm 1.0) \times 10^{-3} \qquad (9)$$

where we have taken into account the unobserved channels $(E \rightarrow \eta\pi^0\pi^0)\pi^0\pi^0$ and $(E \rightarrow \eta\pi^+\pi^-)\pi^+\pi^-$.

The $K\overline{K}\pi$ contribution of the $E$ meson in $\overline{p}p$ annihilation at rest into $K\overline{K}3\pi$ has been measured earlier [1]: $(2.0 \pm 0.2) \times 10^{-3}$. We then find the ratio

$$\frac{B(E \rightarrow K\overline{K}\pi)}{B(E \rightarrow \eta\pi\pi)} = 0.61 \pm 0.19. \qquad (10)$$

The presence of an additional overlapping pseudoscalar around 1490 MeV [6,8], decaying to $K^*\overline{K}$, would, however, modify this ratio. Assuming that $a_0\pi$ contributes 50% to $K\overline{K}\pi$ [1] we also find from eqn. 8 and 9

$$\frac{B(a_0 \to K\overline{K})}{B(a_0 \to \eta\pi)} = 0.54 \pm 0.18, \quad (11)$$

while the corresponding MARK III ratio in radiative $J/\psi$ decay is $1.3 \pm 0.6$ for the lowest state in the $\iota$ structure [6,10]. Our result eqn.11 is in good agreement with the estimate $0.37 \pm 0.07$ determined from other data [27]. However, the uncertainty in the $K^*\overline{K}$ branching ratio (50% according to ref. [1]) is not known and therefore eqn. 11 may have large additional systematic errors. Ultimately, the $K\overline{K}\pi$ decay channel will have to be studied with high statistics data from LEAR.

It is also interesting to combine eqn. 8 with the MARK III result for $\iota \to a_0^{\pm}(\to \eta\pi^{\pm})\pi^{\mp}$ [10] and compare with DM2 data. Using eqn. 8 we predict from MARK III that $B(J/\psi \to \gamma\iota \to \gamma\eta\pi^+\pi^-)$ $= (6.0 \pm 1.3) \times 10^{-4}$ in excellent agreement with DM2: $(7.0 \pm 1.3) \times 10^{-4}$ [9].

Summarizing, we have observed for the first time the $E$ meson decaying to $\eta\pi^+\pi^-$ and $\eta\pi^0\pi^0$ through $a_0(980)\pi$ and $\eta(\pi\pi)_s$ in $\overline{p}p$ annihilation at rest. Our data sample exceeds previous data in $K\overline{K}\pi$ by an order of magnitude. The quantum numbers of the $E$ meson are definitively $0^{-+}$. The observation of the $\eta\pi^0\pi^0$ final state implies that $E$ is isoscalar (C=+1). Mass, width and decay branching ratios are compatible with those of the lower state reported in the $\iota$ structure in radiative $J/\psi$ decay.

## Acknowledgement

We would like to thank the technical staff of the LEAR machine group and of all the participating institutions for their invaluable contributions to the success of the experiment. We acknowledge financial support from the German Bundesministerium für Forschung und Technologie, the Schweizerischer Nationalfonds, the British Particle Physics and Astronomy Research Council, the National Science Research Fund of Hungary (contract No. F014357) and the US Department of Energy (contracts No. DE-FG03-87ER40323, DE-AC03-76SF00098 and DE-FG02-87ER40315). F.H. Heinsius and J. Kisiel benefit from financial support provided by the Alexander von Humboldt Foundation.

## References

[1] P. Baillon et al., Nuovo Cimento **50A** (1967) 393
[2] K. D. Duch et al. (Asterix Collaboration), Z. Phys. **C45** (1989) 223
[3] D.F. Reeves et al., Phys. Rev. **D34** (1986) 1960
[4] Review of Particle Properties , Phys. Rev. **D50** (1994) 1173
[5] D.L. Scharre et al. (Crystal Ball Collaboration), Phys. Lett. **97B** (1980) 329
[6] Z. Bai et al. (MARK III Collaboration), Phys. Rev. Lett. **65** (1990) 2507
[7] J.-E. Augustin et al. (DM2 Collaboration), Phys. Rev. **D46** (1992) 1951
[8] V.G. Ableev et al. (Obelix Collaboration), Proc. LEAP 94 Conf., Slovenia (1994)
[9] J.-E. Augustin et al. (DM2 Collaboration), Phys. Rev. **D42** (1990) 10
[10] T. Bolton et al. (MARK III Collaboration), Phys. Rev. Lett. **69** (1992) 1328
[11] C. Defoix et al., Nucl. Phys. **B44** (1972) 125
[12] T.A. Armstrong et al., Z. Phys. **C52** (1991) 389
[13] E. Aker et al. (Crystal Barrel Collaboration), Nucl. Instr. Methods **A321** (1992) 69
[14] C. Amsler et al. (Crystal Barrel Collaboration), Phys. Lett. **B340** (1994) 259
[15] D. Urner, PhD Thesis, Universität Zürich (unpublished), 1995
[16] C. Amsler et al. (Crystal Barrel Collaboration, Phys. Lett. **B327** (1994) 425
[17] R. Brun et al., GEANT3, CERN Report DD/EE/84-1 (1987)
[18] C. Amsler et al. (Crystal Barrel Collaboration), Phys. Letters **B322** (1994) 431
[19] C. Amsler et al. (Crystal Barrel Collaboration), Phys. Letters **B291** (1992) 347
[20] C. Amsler and J. C. Bizot, Comp. Phys. Com. **30** (1983) 21
[21] K. L. Au, D. Morgan and M.R. Pennington, Phys. Rev. **D35** (1987) 1633
[22] C. Amsler et al. (Crystal Barrel Collaboration), Phys. Lett. **B311** (1993) 362
[23] G. Reifenröther and E. Klempt, Phys. Lett. **B245** (1990) 129
[24] D. Alde et al. (GAMS Collaboration), Phys. Lett. **B177** (1986) 115
[25] G.R. Kalbfleisch, Phys. Rev. **D10** (1974) 916
[26] C. Amsler et al. (Crystal Barrel Collaboration), Phys. Lett. **B333** (1994) 277
[27] C. Amsler, , Proc. XXVII Int. Conf. on HEP, Glasgow, IOP publ. (1995) p. 199